

# A General One-Pot Strategy for the Synthesis of High-Performance Transparent-Conducting-Oxide Nanocrystal Inks for All-Solution-Processed Devices\*\*

Jizhong Song, Sergei A. Kulinich, Jianhai Li, Yanli Liu, and Haibo Zeng\*

**Abstract:** For all-solution-processed (ASP) devices, transparent conducting oxide (TCO) nanocrystal (NC) inks are anticipated as the next-generation electrodes to replace both those synthesized by sputtering techniques and those consisting of rare metals, but a universal and one-pot method to prepare these inks is still lacking. A universal one-pot strategy is now described; through simply heating a mixture of metal–organic precursors a wide range of TCO NC inks, which can be assembled into high-performance electrodes for use in ASP optoelectronics, were synthesized. This method can be used for various oxide NC inks with yields as high as 10 g. The formed NCs are of high crystallinity, uniform morphology, monodispersity, and high ink stability and feature effective doping. Therefore, the inks can be readily assembled into films with a surface roughness of 1.6 nm. Typically, a sheet resistance of  $110 \Omega \text{sq}^{-1}$  can be achieved with a transmittance of 88 %, which is the best performance for TCO NC ink-based electrodes described to date. These electrodes can thus drive a polymer light-emitting diode (PLED) with a luminance of  $2200 \text{cdm}^{-2}$  at  $100 \text{mA cm}^{-2}$ .

Transparent conducting oxide (TCO) nanocrystal (NC) ink-assembled films have received increasing attention as next-generation transparent electrodes (TEs) for optoelectronic devices for two reasons: 1) The TEs that are currently used in classical devices, such as LEDs, are indium tin oxide (ITO) electrodes deposited by vacuum sputtering, but the development of sustainable variants of this process has encountered

serious problems.<sup>[1]</sup> First, indium is a rare metal and hence highly expensive and will be exhausted within ten years. Therefore, searching for more inexpensive and more abundant substitutes, such as electrodes based on Zn, which is 1000 times cheaper than indium and more earth-abundant, is imperative.<sup>[2]</sup> Second, vacuum sputtering technique must be carried out under vacuum and at high operating temperatures, which contrasts with current demands for low-cost displays and light-generation devices as more than half of the amount of ITO is wasted during sputtering.<sup>[1a,3]</sup> In contrast, chemically synthesized NC inks provide various options when selecting oxide matrixes and dopants, such as ZnO doped with aluminum (AZO), gallium (GZO), and indium (IZO), greatly reducing the usage of indium. 2) Flexible, stretchable, and wearable optoelectronic devices have received more and more attention, but these devices require suitable new TEs.<sup>[4]</sup> Obviously, TCO NC inks are compatible with these flexible and stretchable substrates,<sup>[5]</sup> which can be simply prepared by solution-based techniques, such as spin coating, ink-jet printing, spraying, and roll-to-roll production.

However, a one-pot and universal strategy for the fabrication of a wide range of TCO NC inks is still highly desirable. In recent years, the hot-injection method has become very popular for the synthesis of monodisperse colloidal NCs,<sup>[6]</sup> which have been used to prepare ITO and GZO NC inks.<sup>[7]</sup> Nevertheless, such a process involves a chemical reaction between the injected sources and the mother solution and suffers from two disadvantages.<sup>[8]</sup> First, a small dose of injection is usually chosen to achieve high-quality doping, but this injection mode leads to a low throughput and is difficult to scale-up. Second, the doping quality is very sensitive to the dopant element and the injection parameters. All of the parameters have to be changed to prepare oxide NC inks with different dopants.

Herein, we report a facile and universal one-pot method for the synthesis of a wide range of TCO NC inks and the corresponding electrodes for all-solution-processed (ASP) devices with good performances. The proposed approach is generic for various TCOs as well as other oxide (e.g., CoO, MnO, Fe<sub>3</sub>O<sub>4</sub>, CdO) NC inks. The one-pot process can be easily scaled up to 10 g. The TCO NCs are highly crystalline, with a uniform morphology and a narrow size distribution, as well as an effective doping control and a high colloidal stability over one year, making them suitable to be used as inks to print smooth, crack-free, highly transparent, and conductive films. The as-prepared NC electrodes have a surface roughness of 1.6 nm with a resistivity of  $110 \Omega \text{sq}^{-1}$  and a transparency of 88 % for a thickness of 300 nm. These values are the best reported for TCO NC ink-assembled TEs to date,

[\*] J. Z. Song, J. H. Li, Prof. H. B. Zeng  
Institute of Optoelectronics & Nanomaterials  
School of Materials Science and Engineering  
Nanjing University of Science & Technology  
Nanjing 210094 (China)  
E-mail: zeng.haibo@njjust.edu.cn

J. Z. Song, Y. L. Liu, Prof. H. B. Zeng  
School of Materials Science and Engineering and State Key  
Laboratory of Mechanics and Control of Mechanical Structures  
Nanjing University of Aeronautics & Astronautics  
Nanjing (China)

S. A. Kulinich  
Institute of Innovative Science and Technology, Tokai University  
Kanagawa 259-1292 (Japan)  
and  
School of Engineering and Applied Science, Aston University  
Birmingham B4 7ET (UK)

[\*\*] This work was supported through the National 973 project of the National Basic Research Program of China (2014CB931700) and the National Natural Science Foundation of China (61222403).

Supporting information for this article is available on the WWW under <http://dx.doi.org/10.1002/ange.201408621>.

and these electrodes can drive an ASP polymer light-emitting diode (PLED) with a luminance as high as  $2200 \text{ cd m}^{-2}$  at  $100 \text{ mA cm}^{-2}$ .

According to our strategy, the TCO NCs were synthesized through a one-pot heating process of metal–organic precursors in 1-octadecene (ODE) at  $270^\circ\text{C}$  under  $\text{N}_2$  atmosphere. Oleylamine (OAm) and oleic acid (OA) were used as surfactants, and 1-dodecanol (DDL) was employed as a reactant to supply hydroxy groups. When compared with the conventional hot-injection method for the synthesis of oxide NCs, a cheaper alcohol, namely DDL, not the usually employed 1,16-hexadecanediol,<sup>[9]</sup> was used for the esterification reaction (see the Supporting Information, Note S1). Typically, for the synthesis of the IZO NCs, zinc stearate ( $\text{Zn}(\text{St})_2$ , 0.95 mmol), indium(III) acetylacetonate ( $\text{In}(\text{acac})_3$ , 0.05 mmol), ODE (17 mL), OAm (3 mL), OA (1 mL), and DDL (1 mL) were first added to a 100 mL four-neck flask, and the resulting solution was degassed at  $140^\circ\text{C}$  for 30 minutes. After mixing at  $200^\circ\text{C}$  for 30 minutes, the solution was heated to  $270^\circ\text{C}$  in 10 minutes. The mixture was kept at  $270^\circ\text{C}$  for 30 minutes for NC growth.

The chemical reactions taking place during NC formation are presented in Figure 1a. The process consists of two reactions, namely ester elimination and condensation reactions. In detail, the metal precursor molecules (one, two, or more for pure and doped NCs) react with DDL, producing  $\text{M}-\text{OH}$  species through release of ester byproducts. The chemical reactions between the metal–organic precursors and the alcohols and the formation of the  $\text{M}-\text{OH}$  products and the ester byproducts in non-hydrolytic sol–gel reactions have been studied by FTIR spectroscopy.<sup>[6b,10]</sup> During the reaction, OA and OAm molecules behave as surfactants. The kinetics of the ester formation reaction with metal precursors in the presence of OA and OAm have also been studied.<sup>[11]</sup> Subsequently, the formed metal–hydroxide species condensed by releasing  $\text{H}_2\text{O}$  molecules, resulting in the formation of metal oxides. Remarkably, two different  $\text{M}-\text{OH}$  species reacted to form  $\text{M}-\text{O}-\text{M}_1-\text{OH}$ , which eventually formed doped TCO NCs.

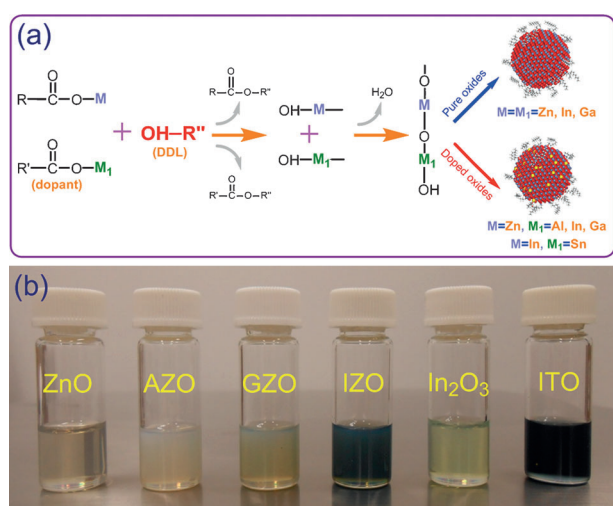


**Figure 1.** The proposed one-pot strategy. a) Synthesis of both pure and doped TCO NCs. b) Photographs of a series of TCO NC inks dispersed in toluene with stabilities of more than one year.

Photographs of various TCO NC inks dispersed in toluene, which are stable for more than one year, are shown in Figure 1b. During the reactions, the carboxy and amine groups in OA and OAm adsorbed or were grafted onto the surface of the NCs. These surface alkyl groups help the NCs to disperse in various organic media as inks with a high stability. When Al, Ga, In, or Sn were incorporated into  $\text{ZnO}$  or  $\text{In}_2\text{O}_3$  NCs, the ink color changed from transparent to milky, green–yellow, and navy blue or from yellow to blue, respectively. The color change verifies the effective doping, arising from the increase in the number of conduction electrons provided by the dopants, which can even induce surface plasmon resonance in the near-infrared region as recently reported.<sup>[12]</sup> The X-ray diffraction (XRD) patterns presented in Figure S1 reveal that the doped  $\text{ZnO}$  and  $\text{In}_2\text{O}_3$  NCs preserve either their hexagonal  $\text{ZnO}$  wurtzite or the basic cubic  $\text{In}_2\text{O}_3$  bixbyite structures, respectively. No additional phases could be found irrespective of the dopants used, indicating that pure phases had been formed. Moreover, aside from for the synthesis of typical TCO NCs, such a general one-pot method can also be used to prepare other metal oxide NCs, such as  $\text{Fe}_3\text{O}_4$ ,  $\text{MnO}$ ,  $\text{CoO}$ , and  $\text{CdO}$  NCs and their doped systems (Figure S2).

The general applicability of our one-pot method for the synthesis of NCs is highlighted in Figure 2. Monodisperse and highly crystalline hexagonal-pyramidal-shaped  $\text{ZnO}$  NCs with a narrow size distribution centered at 12 nm were commonly observed (Figure 2a,b). A high-resolution transmission electron microscopy (HRTEM) image shows the triangular side surfaces and the hexagonal base projection (Figure 2b, inset), revealing the hexagonal pyramidal structure (the structural models are shown in Figure S3). Hexagonal pyramidal NCs with the same exposed crystal facets were recently reported to feature unique electrical properties.<sup>[13]</sup> As shown in Figure 2c–e, doped  $\text{ZnO}$  NCs can be easily obtained through the same procedure. Doping will not influence the crystallinity, monodispersity, morphology, and colloidal stability of the NCs. The highly crystalline nature of the IZO NCs is confirmed by the selected-area diffraction (SAED) pattern in Figure 2e, inset. Moreover, their scanning tunneling electron microscopy (STEM) images and elemental mapping confirm that the In atoms were effectively and uniformly incorporated into the  $\text{ZnO}$  NCs (Figure 2f).

The one-pot approach could also be used to prepare  $\text{Ga}_2\text{O}_3$ ,  $\text{In}_2\text{O}_3$ , and ITO (Figure 2g–j). The preparation of pure  $\text{Ga}_2\text{O}_3$  and  $\text{In}_2\text{O}_3$  NCs (Figure 2g,h) indirectly explains why Ga and In could be effectively incorporated into  $\text{ZnO}$  NCs. Reports on high-quality  $\text{Ga}_2\text{O}_3$  NC inks are very scarce, whereas the potential of  $\text{Ga}_2\text{O}_3$  in optoelectronics (e.g., in LEDs and photodetectors) has led to increasing interest.<sup>[14]</sup> Likewise, high-quality ITO NCs (displayed in Figure 2i,j) can be easily prepared with a morphology almost as pure as for  $\text{In}_2\text{O}_3$  NCs. To the best of our knowledge, this thin film assembled from ITO NCs has the best conductivity ever reported for such films and can thus be widely used as a TE material for ASP devices.

Compared with the hot-injection method, the proposed approach is easier to scale up because of its flexibility, versatility, and the one-pot fabrication process. Figure 2k,l



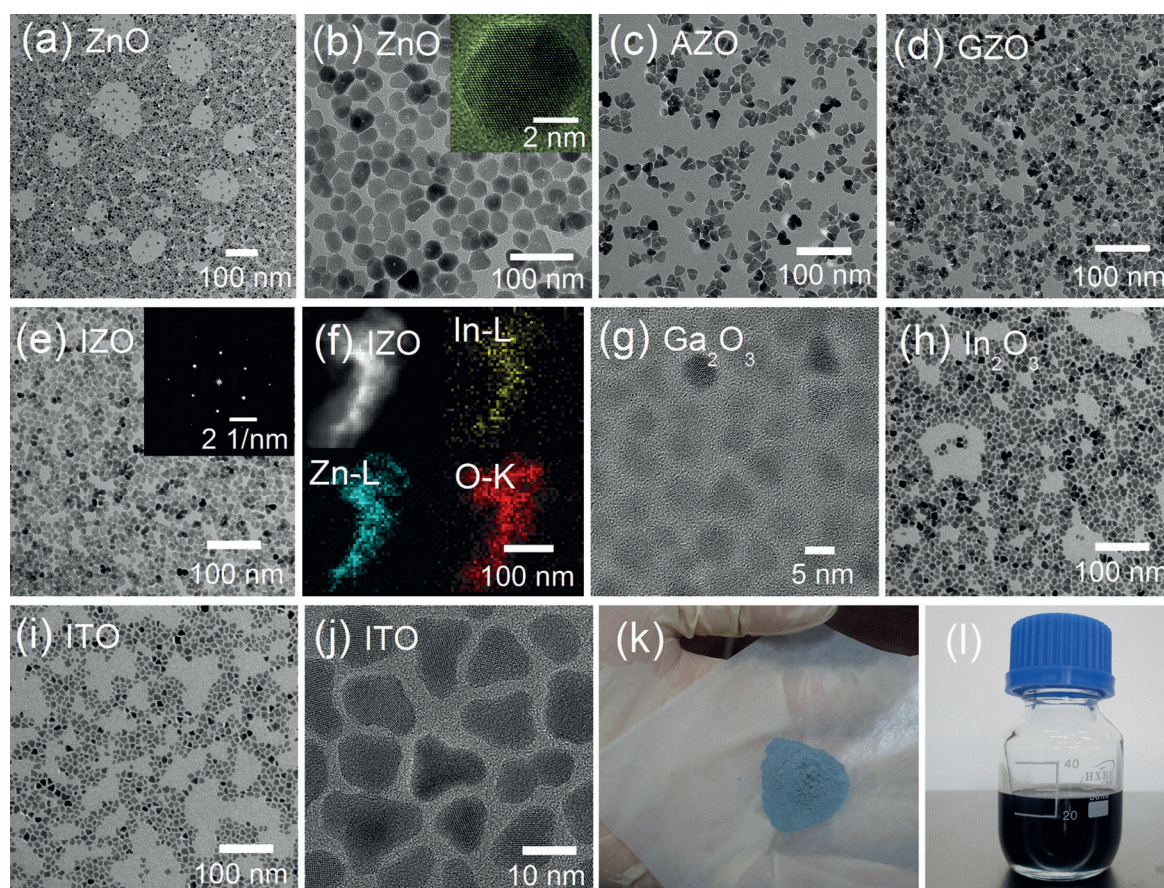


**Figure 2.** Application of this method for the synthesis of various TCO NC inks. a–e) TEM images of ZnO NCs (a,b), AZO (c), GZO (d), and IZO (e). Insets: HRTEM image of one ZnO NC (b), SAED pattern of IZO NCs (e). f) STEM image and elemental mappings of IZO NCs. g–j) TEM images of Ga<sub>2</sub>O<sub>3</sub> NCs (g), In<sub>2</sub>O<sub>3</sub> NCs (h), and ITO NCs (i,j). k) Powder of ITO NCs synthesized on a larger scale (ca. 2.1 g). l) 30 mL of ITO NC ink after redispersion in toluene.

gives an example of a scaled-up synthesis of ITO NCs (Note S2) with a yield of 2.1 g (Figure 2k and Figure S4). Theoretically, for 100% conversion of the precursor into NCs, the mass of NCs is just 1.45 g. The increase in mass is due to the surface OAm and OA molecules, as discussed above and confirmed by IR spectroscopy (Figure S5). The as-synthesized NC powders can be easily redispersed in various organic solvents (Figure 2l). The morphology (Figure S6) is the same as that shown in Figure 2i,j. The mean particle diameter of the ITO NCs after scaling up is  $11 \pm 2.4$  nm with a slightly broadened size distribution (Figure S7). Therefore, the proposed one-pot method is a general approach for synthesizing various TCO NC inks with the possibility of large-scale production, benefiting from the fact that the designed process is insensitive to the local mixing of precursors, which is an obstacle for the scale-up of hot-injection fabrication methods.

Owing to their high crystallinity, uniform morphology, monodispersity, and high stability, these NC inks can be easily assembled into films by mature solution-based processes, such as spin coating. When redispersed in suitable solvents, the NC inks can be used for ASP devices by ink-jet printing or roll-to-roll processing. In this case, the ink consumption will be significantly reduced, which is important when considering the usage of the rare and expensive element In. Using the ITO NC inks obtained in a large amount, we prepared a film with

a thickness of 300 nm. Its transparency and conductivity were very close to those of the film prepared on a smaller scale (Figure S8). This means that the scale-up does not influence the performance of the corresponding TEs.

Taking IZO as a typical example, the as-obtained inks can be easily assembled into NC films (Figure 3). A cross-sectional image of a 150 nm thick film after one cycle of spin coating on glass is shown in Figure 3a. After exposure to UV light for one hour, the second layer was coated (Figure 3b). The two-layer IZO film has a thickness of approximately 300 nm. The UV irradiation was implemented to enhance the film smoothness and conductivity.<sup>[7a,15]</sup> Upon repeating the procedure one more time, a three-layer film with a thickness of approximately 450 nm was obtained (Figure 3c). The large-scale cross-sectional SEM image of the three-layer film in Figure 3d reveals the formation of a dense, uniform, and crack-free film with a very smooth surface, which is also confirmed by the top-view image in Figure 3e. The surface roughness of the film was measured by atomic force microscopy (AFM) and determined to be as small as approximately 1.6 nm (Figure 3f). The quality of the NC ink-assembled films is even comparable to those fabricated by sputtering. Similarly, various high-quality TCO NC films could be successfully obtained (Figure S9). The high-quality inks greatly favor the fabrication of assembled films through

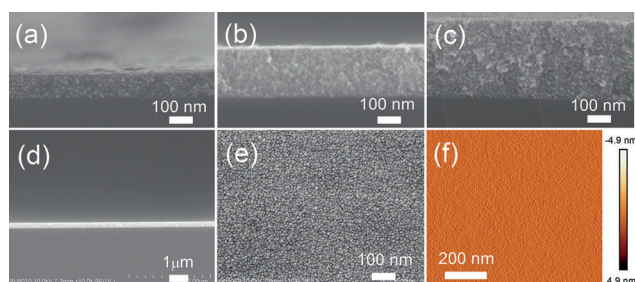


**Figure 3.** High-quality electrodes by assembling NC inks. a–c) Cross-sectional SEM images of IZO NC films obtained by one-layer (a), two-layer (b), and three-layer (c) coatings on glass substrates. d) Large-scale cross-sectional view of the three-layer IZO NC electrode. e) Surface SEM and f) AFM images of three-layer IZO NC electrodes. Surface roughness based on (f): 1.6 nm.

a layer-by-layer procedure, facilitating the adjustment of the thickness, and in turn improving the transparency and conductivity of the films, which is crucial for ASP devices.

The outstanding performances of these NC films are illustrated in Figure 4. The performances of the NC films can be optimized by controlling their thickness (Figure S10a). The two-layer (300 nm thick) film demonstrated the best integrated performance with a low resistance, high transparency, and a smaller amount of the NC inks. Therefore, all of the NC films described in the following were assembled according to the two-layer process. The UV/Vis spectra show that all of the TCO films prepared in this study were highly transparent in the visible range (Figure 4a). The transparency ( $> 80\%$ ) is only slightly lower than that of the glass substrate, which corresponds to the value usually required for the use of TEs in various ASP devices.

The dependence of the conductivity on the doping dose of the NC films is presented in Figure 4b. The optimal doping ratios, corresponding to the lowest resistances, were found to be 1, 3, 5, and 5 at% for AZO, GZO, IZO, and ITO, respectively.<sup>[1c,16]</sup> These results are similar to those obtained for vacuum deposition films. The real doping concentrations in the NCs were systemically measured by energy-dispersive X-ray spectroscopy (EDS), X-ray photoelectron spectroscopy (XPS), and inductively coupled plasma atomic emission spectroscopy (ICP-AES). The doping ratios determined by the different techniques were consistent and slightly higher

than the original ratios shown in Table S1, demonstrating a high doping efficiency. The optimally treated 300 nm thick IZO and ITO films shown in Figure 4b displayed a sheet resistance of as low as 350 and 110  $\Omega\text{sq}^{-1}$ , respectively. The ITO NC film has the best properties ever reported for films deposited by wet-chemistry methods (Figure 4c). These resistance values ( $< 400 \Omega\text{sq}^{-1}$ ), along with a high transparency, already meet the requirements for electrodes used in various ASP devices, including resistive touch panels, displays, and windows.<sup>[1b,4a,5a,7a,17]</sup>

The integrated performances of various TCO NC films prepared by our one-pot method and by other recently reported wet-chemistry methods are compared in Figure 4c.<sup>[7,18]</sup> The top-left corner indicates better integrated performances with a low sheet resistance and a high transparency. On the one hand, the curves of our ITO and AZO materials obviously cross those of previously reported materials, which reveals that our ITO and AZO films have comparable properties to those reported materials. On the other hand, the curves of our IZO and GZO electrodes are located in the upper-left-hand corner. This clearly demonstrates that the performances of our IZO and GZO NC electrodes are better than those reported in previous studies. ITO, with a resistance of 110  $\Omega\text{sq}^{-1}$  and a transparency of 88%, exhibits the best performance. Finally, this is the first report that describes the synthesis of a series of high-performance NC inks by the same one-pot method. Recently, new TEs<sup>[19]</sup> that are based on Cu nanowires (NWs), Ag NWs, graphene, or carbon nanotubes have also exhibited excellent integrated performances (Figure S11). Nonetheless, the low-cost, solution-based process make these TCO NC inks competitive materials for practical applications in a wide range of optoelectronic materials.

The feasibility of applying these NC electrodes in PLEDs is demonstrated in Figure 5. This device is compatible with solution-based techniques, such as roll-to-roll and ink-jet printing. The device structure is presented in Figures S12 and S13. Except for the LiF and Al cathodes, all of the other layers, including our NC electrodes, were sequentially deposited onto a glass substrate through a spin-coating process. Figure 5a shows the normalized EL spectra of the as-prepared PLEDs using our NC film and commercial ITO TEs. Remarkably, the two devices exhibit almost the same electroluminescence

(EL) spectra. This demonstrates the validity of our NC electrodes in ASP devices, which was further verified by the bright and uniform blue light emitted from the whole pixel under a bias of 6 V (Figure 5a, inset). Furthermore, the luminescence brightness and efficiencies of the devices are only slightly lower than those obtained with commercial TEs (Fig-

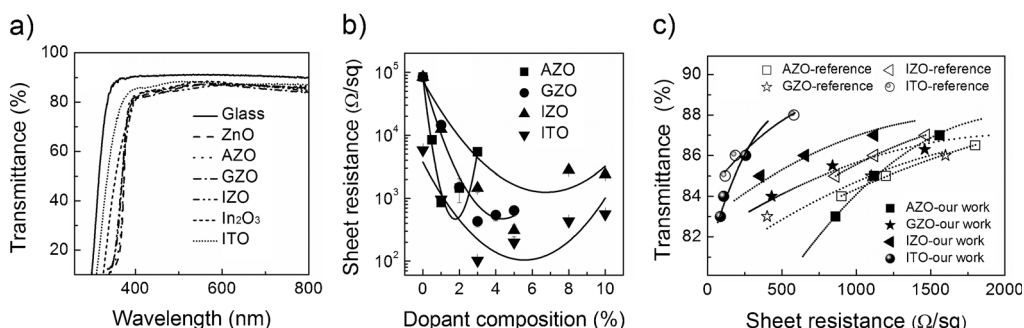


**Figure 4.** Outstanding performances of electrodes assembled from various NC inks. a) Transmittance spectra of NC films coated on glass substrates. b) Dependence of the sheet resistance on the dopant concentration. c) Integrated performances of transmittance and sheet resistance in this study (solid), compared to recently reported results (hollow; AZO, GZO, IZO, and ITO).



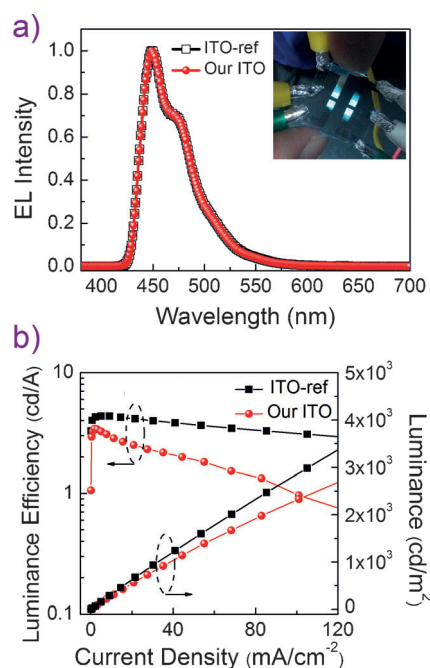


**Figure 5.** PLED device based on ITO NC electrodes. a) EL spectra of PLEDs with TEs from ITO NC inks developed in this study and commercial films. Inset: photograph of the device emitting blue light. b) Luminance efficiency and luminance versus the current density of the devices.

ure 5b and S14). A detailed comparison of the performances is given in Table S2. Typically, the luminance and quantum efficiencies can be as high as  $2200 \text{ cd m}^{-2}$  and 0.91 % at  $100 \text{ mA cm}^{-2}$ , which are almost the same as the values obtained using commercial TEs. These performances further confirm the high quality of the NC inks obtained by our newly developed one-pot strategy.

In summary, a general one-pot method was developed to prepare NC inks of diverse metal oxides through a simple one-pot heating process of metal–organic precursors. The inexpensive alcohol DDL is employed in the fabrication process instead of the widely used 1,2-hexadecanediol. The formed monodisperse NCs are highly crystalline, with a uniform morphology and a high stability. Therefore, they can be assembled into high-quality NC TEs. Typically, the ITO NC TEs with a resistance of  $110 \Omega \text{ sq}^{-1}$  and a transparency of 88 % exhibited the best performance compared to other reported electrodes and could drive PLEDs fabricated by solution-based processes. This is the first report on the preparation of a series of NC inks by a simple one-pot procedure. The proposed method is easily modified for high-throughput production, making the formed NC inks very attractive for applications in a wide range of all-solution-processed, flexible, stretchable, and wearable devices.

Received: August 31, 2014

Published online: November 17, 2014

**Keywords:** nanocrystal inks · nanocrystals · nanostructures · solution processes · transparent conducting oxides

- [1] a) J. Cui, A. Wang, N. L. Edleman, J. Ni, P. Lee, N. R. Armstrong, T. J. Marks, *Adv. Mater.* **2001**, *13*, 1476–1480; b) D. S. Hecht, L. Hu, G. Irvin, *Adv. Mater.* **2011**, *23*, 1482–1513; c) P. D. C. King, T. D. Veal, *J. Phys. Condens. Matter* **2011**, *23*, 334214; d) D. S. Ginley, C. Bright, *MRS Bull.* **2000**, *25*, 15–18.
- [2] a) H. Kim, J. S. Horwitz, S. B. Qadri, D. B. Chrisey, *Thin Solid Films* **2002**, *420*, 107–111; b) J.-H. Kim, H. Lee, S. Choi, K. H. Bae, J. Y. Park, *Thin Solid Films* **2013**, *547*, 163–167.
- [3] a) H. Hong, H. Jung, S.-J. Hong, *Res. Chem. Intermed.* **2010**, *36*, 761–766; b) J. Musil, J. Vlček, *Surf. Coat. Technol.* **1999**, *112*, 162–169.
- [4] a) J. Lewis, S. Grego, B. Chalamala, E. Vick, D. Temple, *Appl. Phys. Lett.* **2004**, *85*, 3450–3452; b) F. Xu, Y. Zhu, *Adv. Mater.* **2012**, *24*, 5117–5122.
- [5] a) H. Wu, D. S. Kong, Z. C. Ruan, P. C. Hsu, S. Wang, Z. F. Yu, T. J. Carney, L. B. Hu, S. H. Fan, Y. Cui, *Nat. Nanotechnol.* **2013**, *8*, 421–425; b) S. Brovelli, N. Chiodini, R. Lorenzi, A. Lauria, M. Romagnoli, A. Paleari, *Nat. Commun.* **2012**, *3*, 690.
- [6] a) Y. F. Chen, M. Kim, G. Lian, M. B. Johnson, X. G. Peng, *J. Am. Chem. Soc.* **2005**, *127*, 13331–13337; b) A. Narayanaswamy, H. F. Xu, N. Pradhan, M. Kim, X. G. Peng, *J. Am. Chem. Soc.* **2006**, *128*, 10310–10319.
- [7] a) E. D. Gaspera, M. Bersani, M. Cittadini, M. Guglielmi, D. Pagani, R. Noriega, S. Mehra, A. Salleo, A. Martucci, *J. Am. Chem. Soc.* **2013**, *135*, 3439–3448; b) J. Lee, S. Lee, G. Li, M. A. Petruska, D. C. Paine, S. Sun, *J. Am. Chem. Soc.* **2012**, *134*, 13410–13414.
- [8] X. Liu, M. T. Swihart, *Nanoscale* **2013**, *5*, 8029–8036.
- [9] a) S. H. Sun, H. Zeng, D. B. Robinson, S. Raoux, P. M. Rice, S. X. Wang, G. X. Li, *J. Am. Chem. Soc.* **2004**, *126*, 273–279; b) Y. F. Yang, Y. Z. Jin, H. P. He, Q. L. Wang, Y. Tu, H. M. Lu, Z. Z. Ye, *J. Am. Chem. Soc.* **2010**, *132*, 13381–13394.
- [10] a) J. Joo, S. G. Kwon, J. H. Yu, T. Hyeon, *Adv. Mater.* **2005**, *17*, 1873–1877; b) J. Park, J. Joo, S. G. Kwon, Y. Jang, T. Hyeon, *Angew. Chem. Int. Ed.* **2007**, *46*, 4630–4660; *Angew. Chem.* **2007**, *119*, 4714–4745; c) X. Zhong, Y. Feng, Y. Zhang, I. Lieberwirth, W. Knoll, *Small* **2007**, *3*, 1194–1199.
- [11] a) D. Ito, S. Yokoyama, T. Zaikova, K. Masuko, J. E. Hutchison, *ACS Nano* **2014**, *8*, 64–75; b) B. M. Tienes, R. J. Perkins, R. K. Shoemaker, G. Dukovic, *Chem. Mater.* **2013**, *25*, 4321–4329.
- [12] a) T. Wang, P. V. Radovanovic, *J. Phys. Chem. C* **2011**, *115*, 406–413; b) R. Buonsanti, A. Llordes, S. Aloni, B. A. Helms, D. J. Milliron, *Nano Lett.* **2011**, *11*, 4706–4710.
- [13] J. Chang, R. Ahmed, H. D. Wang, H. W. Liu, R. Z. Lo, P. Wang, E. R. Waclawik, *J. Phys. Chem. C* **2013**, *117*, 13836–13844.
- [14] a) T. Chen, K. Tang, *Appl. Phys. Lett.* **2007**, *90*, 053104; b) L. Binet, D. Gourier, *J. Phys. Chem. Solids* **1998**, *59*, 1241–1249; c) T. Wang, V. Chirmanov, W. H. M. Chiu, P. V. Radovanovic, *J. Am. Chem. Soc.* **2013**, *135*, 14520–14523.
- [15] Y.-H. Kim, J.-S. Heo, T.-H. Kim, S. Park, M.-H. Yoon, J. Kim, M. S. Oh, G.-R. Yi, Y.-Y. Noh, S. K. Park, *Nature* **2012**, *489*, 128–132.
- [16] T. Minami, *Semicond. Sci. Technol.* **2005**, *20*, S35–S44.
- [17] Y. Leterrier, L. Médico, F. Demarco, J. A. E. Manson, U. Betz, M. F. Escolà, M. K. Olsson, F. Atamny, *Thin Solid Films* **2004**, *460*, 156–166.
- [18] a) K. J. Chen, F. Y. Hung, S. J. Chang, Z. S. Hu, *Appl. Surf. Sci.* **2009**, *255*, 6308–6312; b) E. Hammarberg, A. Prodi-Schwab, C. Feldmann, *J. Colloid Interface Sci.* **2009**, *334*, 29–36.
- [19] a) J. Song, J. Li, J. Xu, H. Zeng, *Nano Lett.* **2014**, *14*, 6298–6305; b) D.-Y. Cho, K. Eun, S.-H. Choa, H.-K. Kim, *Carbon* **2014**, *66*, 530–538; c) M.-S. Lee, K. Lee, S.-Y. Kim, H. Lee, J. Park, K.-H. Choi, H.-K. Kim, D.-G. Kim, D.-Y. Lee, S. Nam, J.-U. Park, *Nano Lett.* **2013**, *13*, 2814–2821; d) J. J. Liang, L. Li, X. F. Niu, Z. B. Yu, Q. B. Pei, *Nat. Photonics* **2013**, *7*, 817–824.